Real-Time Implementation of a PV System Maximum Power Point Tracking Based on the ANN-Backstepping Sliding Mode Control

Rafika El idrissi*‡ ⓘD , Ahmed Abbou* ⓘD , Mohcine Mokhlis* ⓘD , Hicham Bouzakri* ⓘD ,

Yassine El houm * ⓘD

* Electrical Engineering Department, Mohammadia School of Engineers, Mohammed V University in Rabat, Morocco

(rafika.elidrissi@gmail.com, abbou@emi.ac.ma, mohcine1mo@gmail.com, hichambouzakri@research.emi.ac.ma, elhoum.yassine@gmail.com)

‡ Corresponding Author; Rafika El idrissi, Tel: +212649067698, rafika.elidrissi@gmail.com

Abstract- This work presents a real-time implementation of the maximum power point tracking (MPPT) of the PV system using an ANN-BSMC controller. Effectively, this hybrid control consists of double stages, namely: the artificial neural network (ANN) and the backstepping-sliding mode control (BSMC). The first one can predict the optimum voltage corresponding to the maximum power of the PV module while the second one serves for adjusting the duty cycle of the DC/DC boost converter to follow the voltage given. Test-bench components include a 20W PV module, boost converter with a resistive load of 50Ω, current sensor (ACS712ELC-05B), input voltage and designed output voltage sensors of 0-25V and 0-35V voltage range respectively, temperature and irradiation sensors, as well as NI-DAQ 6321 data collection board required to execute the hybrid control. The system stability is proved using Lyapunov functions. The applied approach is compared to the P&O-BSMC in real-time under the same weather conditions. The comparison efficiency was performed under two experimental tests. In both results, the ANN-BSMC shows a high dynamic response in terms of tracking rapidity, oscillation around the MPP, steady-state error, and the PV system efficiency. Based on the results, the ANN-BSMC technique could reach the optimum value in about 0.3s while the P&O-BSMC could reach it until 0.7s. As well as the efficiency of the proposed technique is 93%.

Keywords Real-time implementation, NI-DAQ 6321 data acquisition board, MPPT, ANN, Backstepping sliding mode control.

1. Introduction

Recently, renewable energy is in greater demand because fossil fuels are becoming more expensive, and because they are more environmentally friendly. Among these renewable sources, solar system, known as photovoltaic (PV) system, has interested researchers all over the world [1], [2]. This system is able to convert solar sun into electricity. However, the power generated by this source is varying according to the weather conditions. Therefore, a MPPT is mandatory to improve its efficiency and reduce its cost. A DC/DC converter plays a good role to transfer the PV panel maximum power to the load. The MPP operation can be achieved through adjusting its duty cycle. Buck, buck-boost, boost converters are the most dedicated to track the MPP in some relevant researches [3], [4]. However, boost converter shows its

superiority due to the waveform of input current is non-pulsating [5].

A variety of MPPT techniques classified conventional and unconventional have been developed and improved. Among the conventional ones, there is the perturb and observe (P&O) [6], [7] and the incremental conductance methods (INC) [8]–[10], that depending on the power-voltage characteristic curve, they can obtain maximum power. However, these methods suffer from fluctuation around the MPP, which leads to power loss and the overall system can lose its efficiency.

Other intelligent techniques can be considered effective to track the MPP, namely, Genetic Algorithm (GA) [11], [12],

and Particle Swarm Optimization (PSO) [13], [14]. The main drawbacks of these techniques is that they take time in calculation the MPP and they fail to detect the desired value in some cases of the weather conditions changes. Artificial neural network (ANN) has been reported in different researches [15], [16]. The main advantage of this method is to handle real time nonlinear system problems and fast prediction time of the desired value.

Recently researchers have been developed in MPPT methods considering hybrid methods that combine the previous mentioned algorithms with controllers. In these methods, the first loop generates the optimum reference value and the second loop adjusts the PV panel voltage/current. The main advantage of these methods is the high dynamic, and steady state response improvement. For example, linear controllers was proposed in [17]. However, the nonlinear behavior of the DC/DC converter makes this technique susceptible to excessive ripple, steady state inaccuracy when there is a broad range of environmental condition variations.

On the other side, to increase the robustness and stability of the system against external disturbances such solar irradiation, temperature, and load changes, nonlinear controllers have been developed. In [18], a cascaded two-loop method is employed, in the external loop the P&O was used to generate the suitable PV panel voltage while the sliding mode controller (SMC) was proposed to manage the operation point of the system in the inner loop. This control combination suffered from a chattering phenomenon. In [15], [16] have combined the P&O algorithm and the backstepping control with integral action. This control could not mitigate the steady state error despite the existence of integral action and could handle the external disturbances.

Because the earlier MPPT methods have disadvantages. A cascaded intelligent robust method, both in external and inner loops, is proposed in this paper. An ANN was proposed in the external loop thanks to its aptitude to predict the optimal voltage corresponding to the MPP quickly and without any oscillations in contrary to the conventional algorithms. The inner loop consists of The BSMC, which combines the backstepping and sliding mode controllers. This controller was proposed to mitigate the steady state inaccuracy and the oscillation in wide range of operations.

The suggested MPPT technique's robustness against external disturbances to attain the maximum power of the PV module has been tested on an experimental bench. The test bench consists of a PV module, a boost converter, and a resistive load. The MPPT control has been implemented in Simulink real time in external mode using the NI-DAQ 6321 data acquisition board. The National Instruments (NI) data acquisition system is chosen for the quality and high performance offered by these instruments. The NI DAQ is capable of measuring all signals from sensors. Besides, it is characterised by its rapidity in transferring data, large memory, its ease of use, and it is easy to integrate it with Matlab/Simulink.

Two experiments have been conducted to assess the efficiency of the suggested approach in dealing with the irradiation and temperature fluctuations. The performances of the proposed technique was compared experimentally with the P&O-BSMC technique in terms of steady state inaccuracy, oscillation around the MPP, and other parameters. The experimental findings, in both tests, have shown the superiority of the proposed technique.

The paper is divided into the following sections: The system design is provided in section 2, section 3 presents the system modelling, followed by a description of the suggested MPPT approach in section 4, followed by a discussion of experimental findings in section 5, and finally a conclusion in section 6.

2. The Overall System Scheme

Fig.1 presents the adopted PV system scheme, which consists of a PV module, an adaptation stage, and a resistive load. The adaptation stage consists of a boost converter with the proposed controller based MPPT. Each part in "Fig.1" will be explained separately.
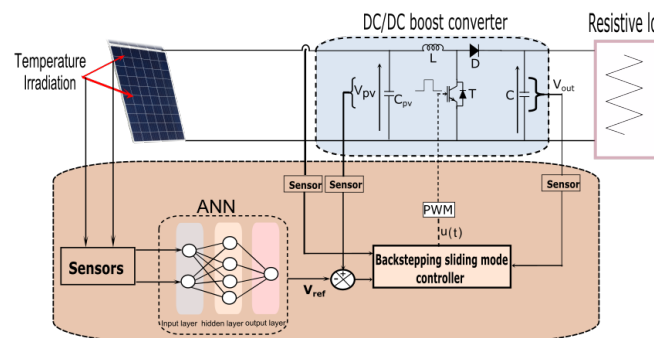
Fig. 1. The global scheme of the applied system.

3. The System Modelling

3.1. PV cell modelling

In order to achieve the necessary output voltage and current, a PV module consists of a number of PV cells that are linked in series and parallel. "Fig.2" shows an ideal PV cell model with a current source linked in parallel to a diode, as well as two resistances connected in parallel and series to present the losses [17, 18].
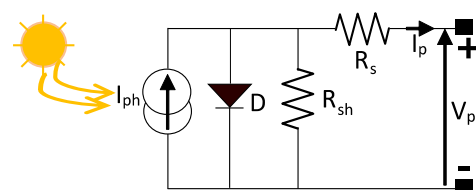
Fig. 2. The PV cell dynamic circuit.

In order to simplify the model, both Rs and Rsh might be ignored as they are equal to zero [23]. The following equations can be used to describe the electrical properties of the PV modules [20, 21].

$$I_p = I_{ph} - I_o \left[exp\left(\frac{qV_p}{\gamma NKT} \right) - 1 \right] \qquad (1)$$

Where Ip [A] and Vp[V] are the PV module output current and voltage respectively, q is the electron charge equals to 1.6×10^{-19} [C], T [°K] is the temperature of the cell, γ s the ideality factor, and K is the Boltzmann constant equals to 1.3805×10^{-23} J/K. The PV Module utilized has N=36 PV cells linked in series.

In "Eq. (2)", the cell saturation current $I_o [A]$ is defined as:

$$I_o = I_{or} \left(\frac{T}{T_r} \right)^3 exp\left(\frac{qE_g}{K\gamma} \left[\frac{1}{T_r} - \frac{1}{T} \right] \right) \qquad (2)$$

Where T_r °K] is the cell nominal temperature, and E_g s the cell's semiconductor band gap equals to 1.1 [eV].

In "Eq. (3)", the cell saturation current at the nominal temperature as follows:

$$I_{or} = \frac{I_{scr}}{exp\left(\frac{qV_{oc}}{N_s K\gamma T} \right) - 1} \qquad (3)$$

In this case, $I_{scr} [A]$ and $V_{oc} [V]$ refer to the short-circuit current at T_r nd the open circuit voltage, respectively.

$I_{ph} [A]$ s the photocurrent that can be expressed as follows:

$$I_{ph} = \left[I_{scr} + K_i (T - T_r) \right] \frac{E}{1000} \qquad (4)$$

K_i A/K] and E [W/m2] are short-circuit current temperature coefficient equals to 4×10^{-4} and the sun irradiation respectively.

The PV module transferred energy to the load can be affected by the weather conditions. To transfer the PV module full energy, regulation of PV module voltage must be done in order to achieve the maximum operating point.

3.2. Modelling of the DC/DC Step-up Converter

The step-up converter is used as interface between the PV module and the load in the system. It is responsible for maximizing the PV module power. Therefore, the control of this converter is mandatory. Assuming the boost converter is working in conductance continuous mode (CCM), the dynamic modelling of this converter passes through two modes of operation. In mode 1, the switch T is on and the diode D is reverse biased (not conducting). By applying the Kirchhoff's law to the circuit of "Fig. 1", we get:

$$\begin{cases} V_{Cpv} = I_{pv} - I_L \\ V_L = V_{pv} \\ V_{Cout} = -I_{out} \end{cases} \qquad (5)$$

In mode 2, the switch T is off and diode D is forward biased (conducting). According to Kirchhoff's law:

$$\begin{cases} V_{Cpv} = I_{pv} - I_L \\ V_L = V_{pv} - V_{out} \\ V_{Cout} = I_L - I_{out} \end{cases} \qquad (6)$$

Using the inductor's volt-second balance and the capacitor's charge balance, the average model of the boost converter in both operation switches is as follows:

$$\begin{cases} \frac{dV_{pv}}{dt} = \frac{1}{C_{pv}} \left(I_{pv} - I_L \right) \\ \frac{dI_L}{dt} = \frac{1}{L} \left(V_{pv} - (1-u) V_{out} \right) \\ \frac{dV_{out}}{dt} = \frac{1}{C_{out}} \left((1-u) I_L - I_{out} \right) \end{cases} \qquad (7)$$

4. The suggested control based MPPT of the implemented PV system

The suggested MPPT control is shown in "Fig.1". This control consists of two stages. In the first one, the ANN is suggested to generate the PV module optimum voltage. In the second one, the BSMC is used to enforce the PV module voltage to follow the provided voltage.

4.1. ANN based MPPT

In recent years, ANNs have been explored as an alternate approach to deal with complicated, nonlinear systems. ANNs do not require any information on the system, which proves their advantage to avoid complicated mathematic calculations. Input and output are recognized based on previously recorded data. The weather conditions (irradiations, temperature) are applied as input parameters to ANN. At the output stage, the PV module optimum voltage is generated to the BSMC to control the boost converter, which drives the PV module voltage to the optimal voltage.

The input layer is supplied with input data, the hidden layer includes many sigmoid hidden neurons receiving data from the input layer and forwarding it to the output layer with linear neurons, which provides the output to the system.

The output activation function of the hidden layer neurons, whose activation function is sigmoid function, are measured using the following relationship:

$$y_j^h = f\left(\sum_{i=1}^{N} W_{ji} X_i + \theta_j^h \right) \qquad (8)$$

Whereas the output layer contains one neuron, whose activation function is linear, uses the following relationship to provide the measured optimal voltage $\hat{V}_{mp}$:

$$y_k^o = f\left(\sum_{j=1}^{Nh} W_{jk} y_j^h + \theta_k^o\right) \qquad (9)$$

In order to implement the ANN, nnstart tool in Matlab was used. Experimental dataset was taken from the used PV module in real-time by changing the irradiation and temperature each time and the optimal voltage was measured at each change of the input data. The number of hidden neurons was chosen 50. The neural network was trained offline using the bayezian-regularization backpropagation algorithm. This algorithm was chosen due to its robustness against difficult, small, and noisy datasets. In our case, we have small dataset composed of 15 patterns of irradiation, temperature, and the corresponding MPP voltage. Therefore, the chosen algorithm was suitable to have best performances. So far, the mean squared error (MSE) is minimized expressed by the following equation:

$$E = \frac{1}{n}\sum_{i=1}^{n}\left(V_{mp}(i) - \hat{V}_{mp}(i)\right)^2 \qquad (10)$$

Where Vmp is the ith target and $\hat{V}_{mp}$ is the estimated output.

The MSE is provided in fig.3 based on the experimental datasets given in "Fig.4". The best MSE during the training process equals to 0.42408, which is quite small. It can be minimized more if we will add more data.
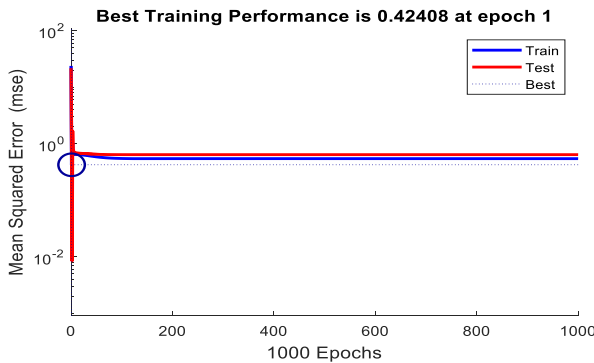
Fig. 3. The performed mean squared error (MSE).
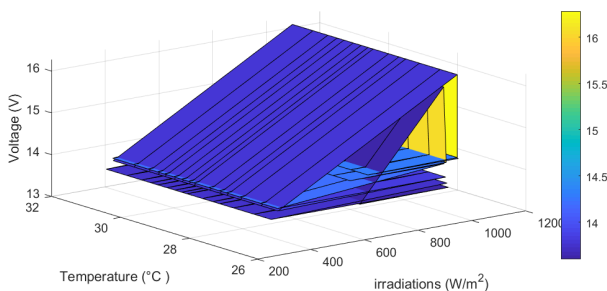
Fig. 4. The experimental used data set.

4.2. Backstepping sliding mode control for MPPT design

Here the backstepping and sliding mode controllers are combined to perform a robust control against the weather conditions changes. The basic principle of this control is to reduce the steady-state inaccuracy of the backstepping control and to eliminate the chattering phenomena of the SMC. This control is intended to force the PV module voltage to follow the voltage provided by the ANN. The design procedures of this controller are as follows:

Firstly, the tracking error has to be defined as follows:

$$e_1 = V_{pv} - V_{ref} \qquad (11)$$

Where Vref is the PV module optimum voltage provided by the ANN. For making the error converging to zero, let us take the time derivative of "Eq. (11)" and considering the "Eq. (7)", yields:

$$\dot{e}_1 = \dot{V}_{pv} - \dot{V}_{ref} = \frac{1}{C_{pv}}\left[i_{pv} - i_L\right] - \dot{V}_{ref} \qquad (12)$$

To check if the tracking error is converged to zero a lyapunov function was chosen as follows:

$$V_1 = \frac{1}{2}e_1^2 \qquad (13)$$

The time derivative of this function using "Eq. (12)" yields:

$$\dot{V}_1 = e_1\dot{e}_1 = e_1\left[\frac{1}{C_{pv}}\left(i_{pv} - i_L\right) - \dot{V}_{ref}\right] \qquad (14)$$

For the lyapunov function to be negative, let us put:

$$\frac{1}{C_{pv}}\left[i_{pv} - i_L\right] - \dot{V}_{ref} = -K_1 e_1 \qquad (15)$$

"Eq. (14)" becomes:

$$\dot{V}_1 = -K_1 e_1^2 \qquad (16)$$

Considering iL as a virtual control, we get:

$$\alpha = i_L = K_1 C_{pv} e_1 + i_{pv} - C_{pv}\dot{C}_{pv}\dot{V}_{ref} \qquad (17)$$

Considering a second error as follows:

$$e_2 = i_L - \alpha \qquad (18)$$

If we replace i_L ith $e_2 + \alpha$ in Equation (14), we obtain the following:

$$\dot{V}_1 = -\frac{e_1 e_2}{C_{pv}} - K_1 e_1^2 \qquad (19)$$

To guarantee the convergence of the second error a second Lyapynov function has to be defined in the following equation:

$$V_2 = V_1^2 + \frac{1}{2}S^2 \tag{20}$$

Where the sliding surface was chosen as follows:

$$S = e_2 \tag{21}$$

The time derivative of this function becomes:

$$\dot{V}_2 = \dot{V}_1 + S\dot{S} = -K_1 e_1^2 + S\left[-\frac{e_1}{C_{pv}} + \dot{S} \right] \tag{22}$$

In order that the stability of the system is guaranteed, we select:

$$\left[-\frac{e_1}{C_{pv}} + \dot{S} \right] = -K_2 S - K_3 \text{sign}(S) \tag{23}$$

Where K2 and K3 are positive defined. The following control input is deduced from "Eq. (22)":

$$u = \frac{L}{V_{out}}\left[-K_2 S - K_3 \text{sign}(S) + \frac{e_1}{C_{pv}} + \frac{1}{L}\left(V_{out} - V_{pv} \right) - \dot{\alpha} \right] \tag{24}$$

Which leads to "Eq. (25)":

$$\dot{V}_2 = -K_1 e_1^2 - \left(K_2 S^2 + K_3 \text{sign}(S) \right) < 0 \tag{25}$$

According to the prior study, the system is stable. Errors converge to zero, resulting in convergence of V_{pv} to V_{ref}.

5. Experimental prototype

The experiment is performed using a prototype, which includes the following hardware:
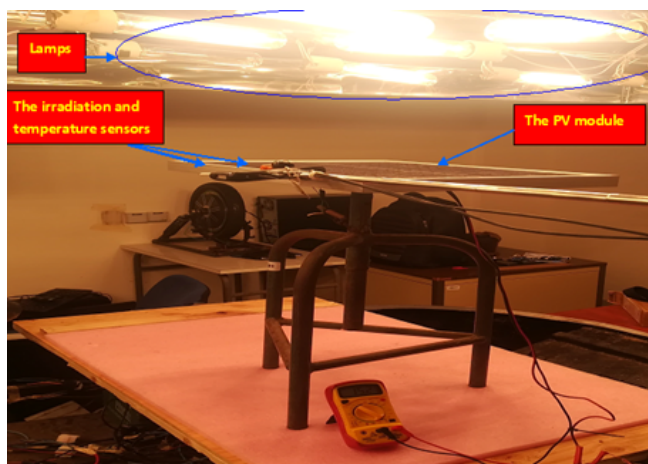
(a)
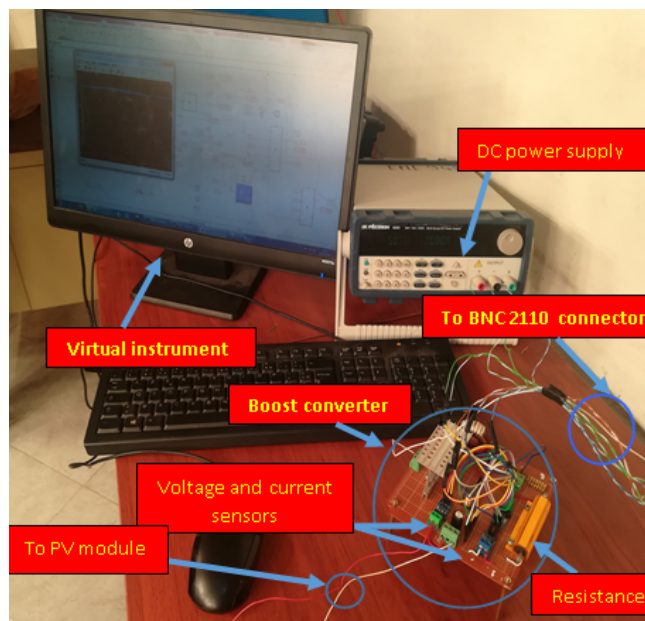
(b)
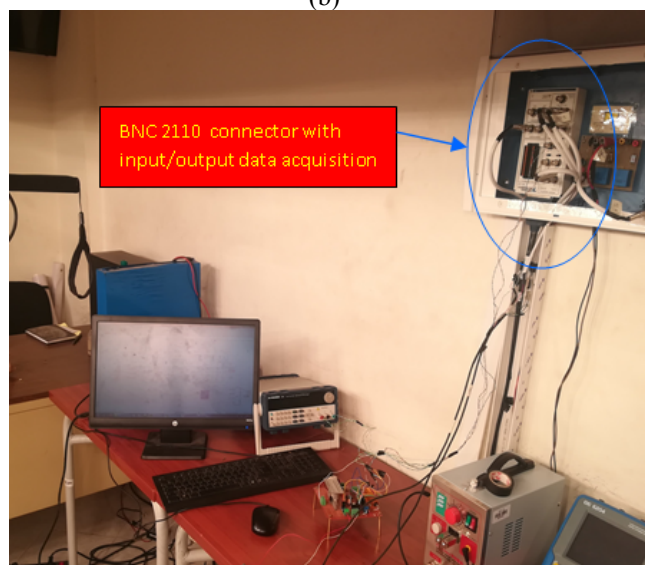
(c)

Fig. 5. The experimental test bench: (a) the left view, (b) the test bench , (c) the right view.

Using Matlab-Simulink in a real-world environment, experimental findings are provided as test 1 and test 2 on PV system to evaluate the efficacy of the proposed controller. The main specifications of the adopted system are listed in "Table 1." and "Table 2."

Table 1. The used PV Module electrical characteristics (SP20-36P)

Parameters	Values
Maximum power (Pm)	20 W
Maximum voltage (Vmp)	17.3 V
Maximum current (Imp)	1.16 A
Short-circuit current (Isc)	1.26 A
Open-circuit voltage (Voc)	21.7 V

Table 2. The designed boost and controller parameters

Parameters	Values
Inductor	0.66 mH
Input capacitor	470 µF
Output capacitor	220 µF
Load resistance	50 Ω
Switching frequency	64 Khz
K1	6×10^5
K2	100
K3	1000

A NI-DAQ 6321 data acquisition board was used to execute the ANN-BSMC controller and generate the PWM signal. The NI-DAQ receives the analogue data through the BNC 2110 connector board using current sensor (ACS712ELC-05B), input and output voltage sensors of 0-25 V and 0-35 V ranges respectively as well as irradiation (Apogee SP-215) and temperature (Apogee ST-100) sensors to be converted into digital values for the digital controller in Matlab/Simulink. The NI-DAQ's PWM module delivers the driving signal to the boost converter's switch to conduct the MPPT. The boost converter switching frequency was chosen equals to 64 KHz as well as the sampling time at 2ms. Low-pass filters have been used to reduce the unwanted noises coming from current and voltage measurement. After these filters, the gains are used to restore the real measured values by the sensors. "Fig.6" depicts the implementation scheme of the proposed techniques in Matlab/Simulink environment to upload the PWM signal into the NI-DAQ board.
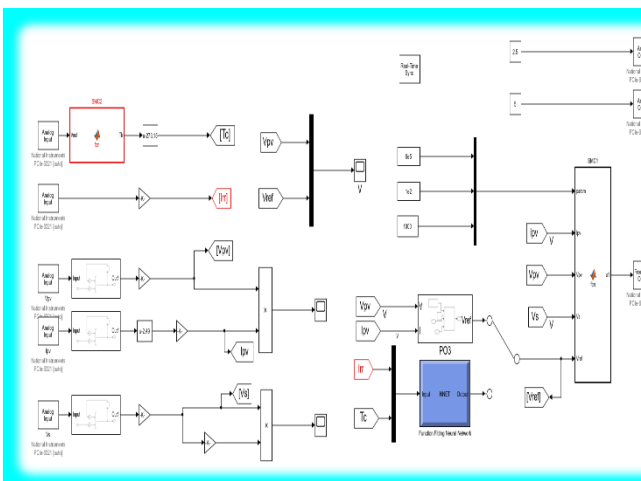
Fig. 6. NI-DAQ implementation scheme of the suggested MPPT techniques.

5.1. The performed Test 1

When the PV system is subjected to a changeable weather conditions, the previously defined controller strategy is implemented in real time using Matlab/Simulink real time desktop in external mode, which is employed to upload it into the NI-DAQ 6321 board as depicted in "Fig.6". The performances of the ANN-BSMC are discussed comparing

them to the P&O-BSMC in real time. Under the given irradiation and temperature from the used sensors in "Fig.7", the experimental results show that both the compared techniques are tracking the MPP.

Although, in "Fig.9", the PV voltage produced by the ANN-BSMC exhibits better tracking performances compared to the P&O-BSMC that exhibits a significant oscillations around the MPP as well as a considerable rise time. The proposed technique tracks the optimum voltage quickly compared to P&O-BSMC; it could reach the optimum value in about 0.3s while the P&O-BSMC could reach it until 0.7s. In addition, "Fig.8" shows that the control law of the ANN-BSMC presents less oscillation compared to the P&O-BSMC. Moreover, as observed in "Fig.10", the power produced by the proposed controller is much higher with reduced oscillations compared to the P&O-BSMC. Therefore, the wasting power is reduced by the proposed technique. Elsewhere, the experimental load power response is shown in "Fig.11". In fact, an undeniable smooth power is guaranteed for feeding the load in case of the ANN-BSMC. Therefore, the ANN-BSMC improves suitably the power quality. A little discrepancy can be seen between the PV module power in "Fig.10" and the load power in "Fig.11", which is attributable to the system losses.

(a)

(b)
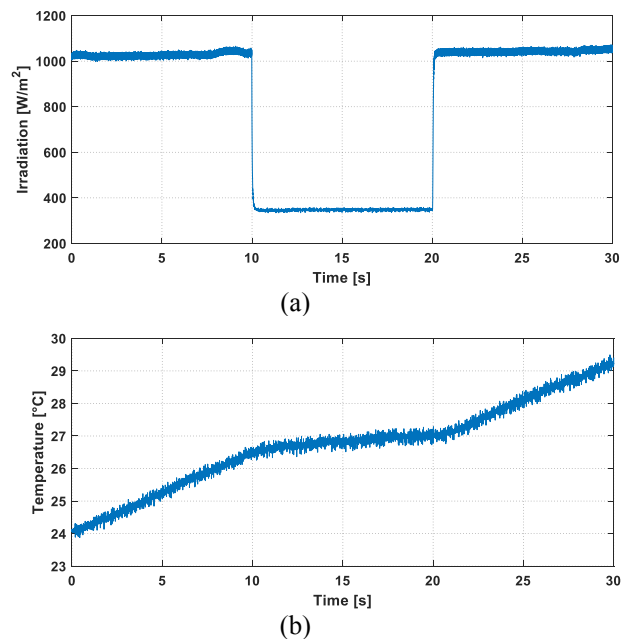
Fig. 7. Measured irradiation (a) and temperature (b).
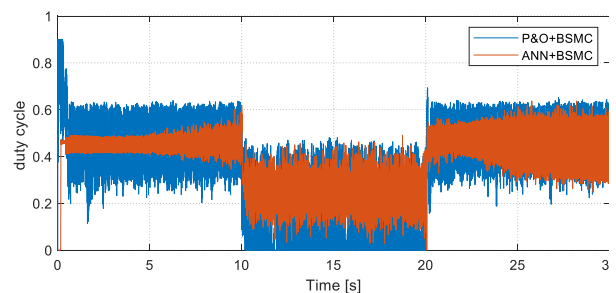
Fig. 8. The duty cycle.
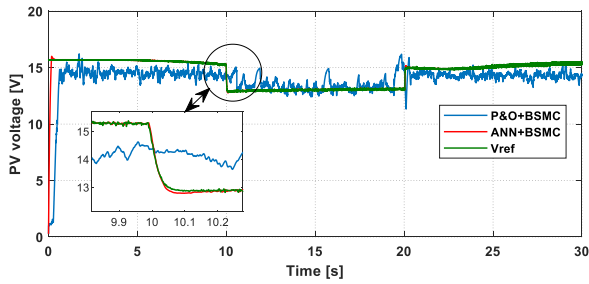
Fig. 9. The PV module output voltage.
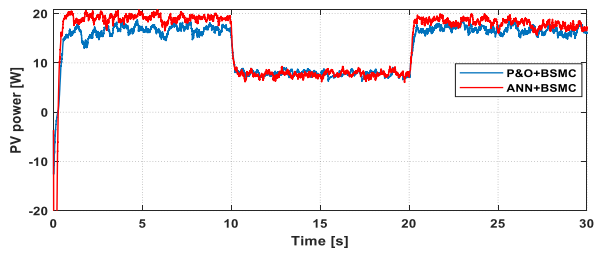
Fig. 10. The PV module output power.
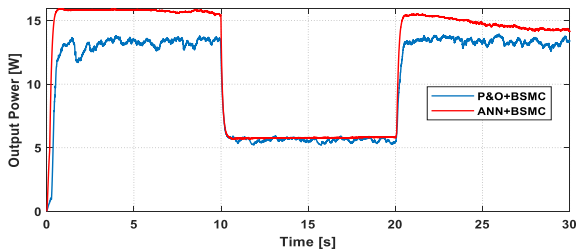
Fig. 11. The load power.

5.2. The performed Test 2

In this test, we switched between the two techniques in real time in order to avoid the mismatch in the testing system conditions. Both techniques are tested simultaneously, using a manual switch, under irradiations of 350 W/m2 and 1000 W/m2 as depicted in "Fig.12". The experimental waveforms of the PV voltage "Fig.13", the PV power "Fig.14", the duty cycle "Fig.15", and the load power "Fig.16" extracted by the ANN-BSMC technique in the two switching conditions confirm the effectiveness of the proposed technique as the MPPT is successfully identified and load power is improved without oscillations. We can say that the experimental results show an undeniable outperformance of the ANN-BSMC technique, which could improve all the performances measures. "Table .3" gives comparison of the proposed techniques.
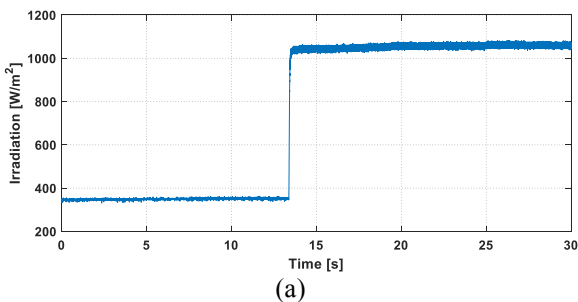
(a)
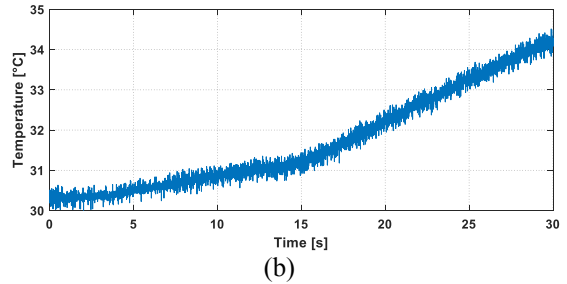
(b)

Fig. 12. Experimental measured profile of irradiation (a) and temperature (b).
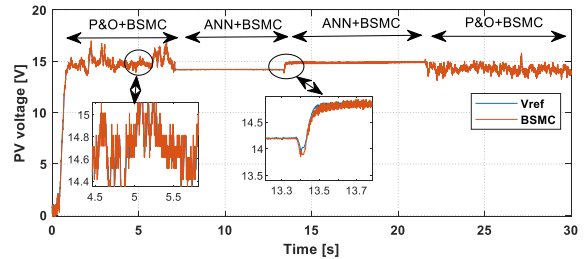
Fig. 13. The experimental PV module voltage response.
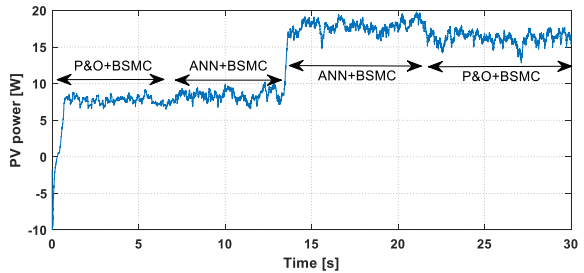
Fig. 14. The experimental PV module power response.
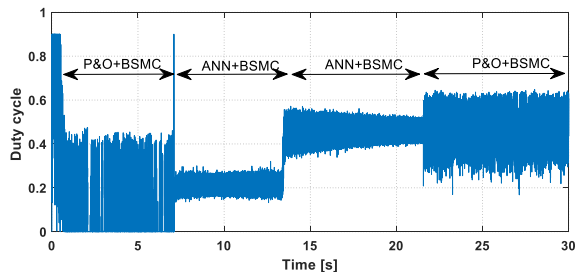
Fig. 15. The duty cycle.
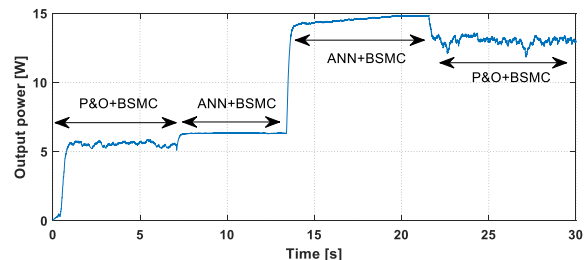
Fig. 16. The load power response.

Table 3. Comparison of the controllers' performances at 1000W/m^2

	Tracking speed(s)	Efficiency (%)	Settling time (s)
ANN-BSMC	0.3	93	0.43
P&O-BSMC	0.7	84	0.64

6. Conclusion

This study focused on an experimental test of the robust ANN-BSMC technique for a PV system in order to prove its tracking performances in real-time. The applied experimental test-bench consists of a PV module of 20W, a boost converter, and a resistive load of 50 ohm with 100W maximal dissipated power. The proposed technique was implemented in Matlab/Simulink in external mode using NI-DAQ 6321 data acquisition board. Based on the given real time experimental results of the performed tests, the ANN-BSMC strategy successfully handled the irradiation and temperature changes and provided several advantages including quick convergence to the optimum value, precision in identifying the MPP, and decreased steady-state oscillations. As a result, the PV system quality has been appropriately improved. This was confirmed by the comparison with the P&O-BSMC technique; in both tests, the ANN-BSMC outperformed the P&O-BSMC technique.

In the future work the implementation of this controller will be applied to the PV system connected to the grid.

References

[1] H. Bouzakri and A. Abbou, "Mono-axial solar tracker with equatorial mount, for an improved model of a photovoltaic panel," *Int. J. Renew. Energy Res.*, vol. 10, no. 2, pp. 578–590, 2020.

[2] H. Bouzakri, A. Abbou, K. Tijani, and Z. Abousserhane, "Biaxial Equatorial Solar Tracker with High Precision and Low Consumption: Modelling and Realization," *Int. J. Photoenergy*, vol. 2021, 2021.

[3] R. El Idrissi, A. Abbou, and M. Mokhlis, "Backstepping Integral Sliding Mode Control Method for Maximum Power Point Tracking for Optimization of PV System Operation Based on High-Gain Observer," *Int. J. Intell. Eng. Syst.*, vol. 13, no. 5, 2020.

[4] K. Osmani, A. Haddad, T. Lemenand, B. Castanier, and M. Ramadan, "An investigation on maximum power extraction algorithms from PV systems with corresponding DC-DC converters," *Energy*, vol. 224, p. 120092, Jun. 2021.

[5] M. Salimi, "Practical implementation of the Lyapunov based nonlinear controller in DC- DC boost converter for MPPT of the PV systems," *Sol. Energy*, vol. 173, no. July, pp. 246–255, 2018.

[6] R. Alik and A. Jusoh, "An enhanced P&O checking algorithm MPPT for high tracking efficiency of partially shaded PV module," *Sol. Energy*, vol. 163, pp. 570–580, Mar. 2018.

[7] S. Thakran, J. Singh, R. Garg, and P. Mahajan, "Implementation of PO Algorithm for MPPT in SPV System," in *2018 International Conference on Power Energy, Environment and Intelligent Control, PEEIC 2018*, 2019, pp. 242–245.

[8] A. Loukriz, M. Haddadi, and S. Messalti, "Simulation and experimental design of a new advanced variable step size Incremental Conductance MPPT algorithm for PV systems," *ISA Trans.*, vol. 62, pp. 30–38, May 2016.

[9] D. Sera, L. Mathe, T. Kerekes, S. V. Spataru, and R. Teodorescu, "On the perturb-and-observe and incremental conductance mppt methods for PV systems," *IEEE J. Photovoltaics*, vol. 3, no. 3, pp. 1070–1078, 2013.

[10] Abdelhakim Belkaid, Ilhami Colak, Korhan Kayisli, and Ramazan Bayindir, "Design and Implementation of a Cuk Converter Controlled by a Direct Duty Cycle INC-MPPT in PV Battery System | Belkaid | International Journal of Smart Grid - ijSmartGrid," *Int. J. Smart Grid*, vol. 3, no. 1, pp. 19–25, 2019.

[11] P. Megantoro, Y. D. Nugroho, F. Anggara, Suhono, and E. Y. Rusadi, "Simulation and characterization of genetic algorithm implemented on MPPT for PV system under partial shading condition," in *Proceedings - 2018 3rd International Conference on Information Technology, Information Systems and Electrical Engineering, ICITISEE 2018*, 2018, pp. 74–78.

[12] M. Tanaka, H. Eto, Y. Mizuno, N. Matsui, and F. Kurokawa, "Genetic algorithm based optimization for configuration and operation of emergency generators in medical facility," in *2017 6th International Conference on Renewable Energy Research and Applications, ICRERA 2017*, 2017, vol. 2017-January, pp. 919–924.

[13] F. M. De Oliveira, S. A. Oliveira Da Silva, F. R. Durand, L. P. Sampaio, V. D. Bacon, and L. B. G. Campanhol, "Grid-tied photovoltaic system based on PSO MPPT technique with active power line conditioning," *IET*, vol. 9, no. 6, pp. 1180–1191, May 2016.

[14] A. I. Nusaif and A. L. Mahmood, "MPPT Algorithms (PSO, FA, and MFA) for PV System Under Partial Shading Condition, Case Study: BTS in Algazalia, Baghdad," *Int. J. Smart Grid-ijSmartGrid*, vol. 4, no. 3, pp. 100–110, 2020.

[15] H. Rezk and E. S. Hasaneen, "A new MATLAB/Simulink model of triple-junction solar cell and MPPT based on artificial neural networks for photovoltaic energy systems," *Ain Shams Engineering Journal*, vol. 6, no. 3. pp. 873–881, 2015.

[16] I. Chtouki, P. Wira, M. Zazi, B. Collicchio, and S. Meddour, "Design, implementation and comparison of several neural Perturb and Observe MPPT methods for photovoltaic systems," *Int. J. Renew. Energy Res.*, vol. 9, no. 2, pp. 757–770, 2019.

[17] R. Abdelrassoul, Y. Ali, and M. S. Zaghloul, "Genetic Algorithm-Optimized PID Controller for Better Performance of PV System," in *Proceedings - 2016 World Symposium on Computer Applications and Research, WSCAR 2016*, 2016, pp. 18–22.

[18] O. P. Pahari and B. Subudhi, "Integral sliding mode-improved adaptive MPPT control scheme for suppressing grid current harmonics for PV system," *IET Renew. Power Gener.*, vol. 12, no. 16, pp. 1904–1914, Dec. 2018.

[19] E. I. Rafika, A. Abbou, M. Mohcine, and M. Salimi, "A comparative study of MPPT controllers for photovoltaic pumping system," in *2018 9th International Renewable Energy Congress, IREC 2018*, 2018, pp. 1–6.

[20] M. Arsalan, R. Iftikhar, I. Ahmad, A. Hasan, K. Sabahat, and A. Javeria, "MPPT for photovoltaic system using nonlinear backstepping controller with integral action," *Sol. Energy*, vol. 170, pp. 192–200, Aug. 2018.

[21] D. Rekioua and E. Matagne, "Optimization of photovoltaic power systems: Modelization, Simulation and Control," *Green Energy Technol.*, vol. 102, 2012.

[22] E. I. Rafika, A. Abbou, S. Rhaili, and M. Salimi, "Maximum power point tracking of photovoltaic systems using backstepping controller," in *Proceedings of 2017 International Conference on Engineering and Technology,*

ICET 2017, 2018, vol. 2018-January, pp. 1–6.

[23] M. Guisser, A. El-Jouni, and E. H. Abdelmounim, "Robust sliding mode MPPT controller based on high gain observer of a photovoltaic water pumping system," *Int. Rev. Autom. Control*, vol. 7, no. 2, pp. 225–232, 2014.

[24] M. Guisser, E. Abdelmounim, M. Aboulfatah, and A. EL-Jouni, "Nonlinear Observer-Based Control for Grid Connected Photovoltaic System," *IOSR J. Electr. Electron. Eng.*, vol. 9, no. 5, pp. 40–52, 2014.

[25] R. El Idrissi, A. Abbou, M. Mokhlis, and M. Salimi, "Adaptive Backstepping Controller Design Based MPPT of the Single-Phase Grid-Connected PV System," *Int. J. Intell. Eng. Syst.*, vol. 14, no. 3, p. 2021.